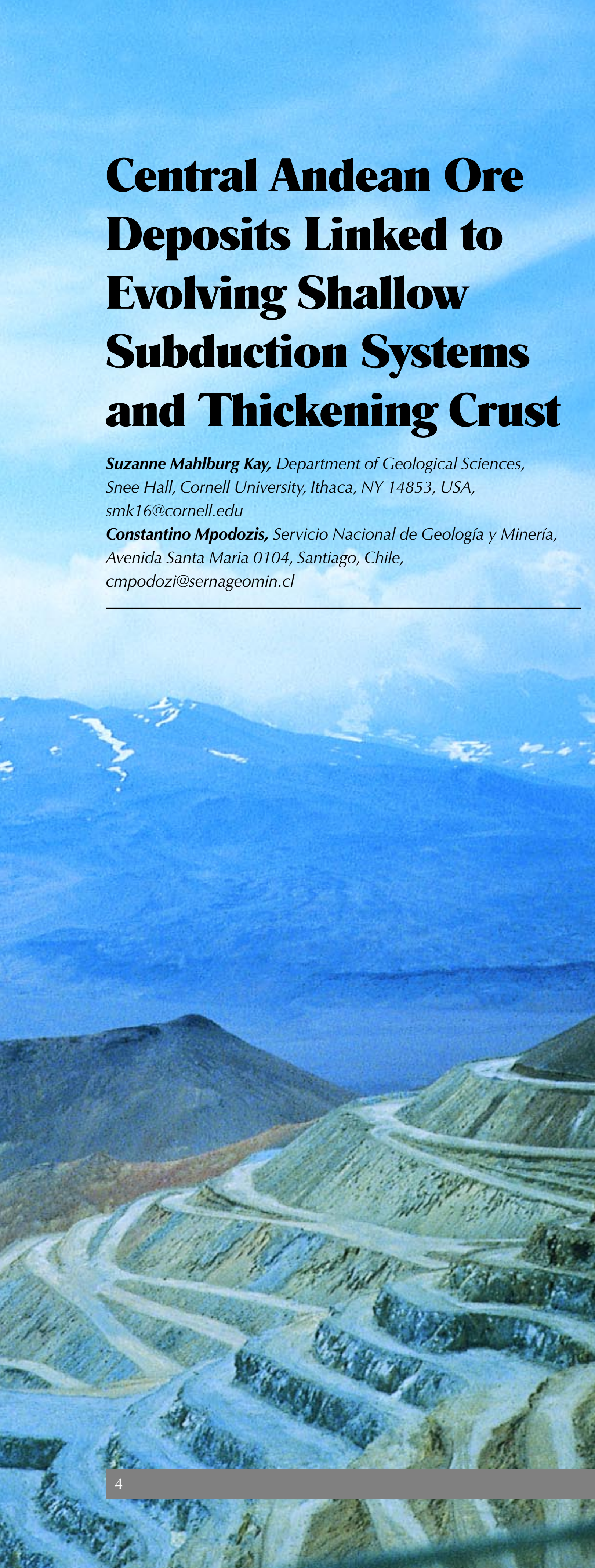

Central Andean Ore Deposits Linked to Evolving Shallow Subduction Systems and Thickening Crust

Suzanne Mahlburg Kay, *Department of Geological Sciences, Snee Hall, Cornell University, Ithaca, NY 14853, USA, smk16@cornell.edu*

Constantino Mpodozis, *Servicio Nacional de Geología y Minería, Avenida Santa Maria 0104, Santiago, Chile, cmpodozi@sernageomin.cl*

ABSTRACT

Major Miocene central Andean (lat 22°–34°S) ore districts share common tectonic and magmatic features that point to a model for their formation over a shallowing subduction zone or during the initial steepening of a formerly flat subduction zone. A key ingredient for magmatism and ore formation is release of fluids linked to hydration of the mantle and lower crust above a progressively shallower and cooler subducting oceanic slab. Another is stress from South American–Nazca plate convergence that results in crustal thickening and shortening in association with magma accumulation in the crust. Fluids for mineralization are released as the crust thickens, and hydrous, lower crustal, amphibole-bearing mineral assemblages that were stable during earlier stages of crustal thickening break down to dryer, more garnet-bearing ones. Evidence for this process comes from trace-element signatures of pre- to postmineralization magmas that show a progression from equilibration with intermediate pressure amphibole-bearing residual mineral assemblages to higher pressure garnet-bearing ones. Mineralization over the shallowing subduction zone in central Chile (28°–33°S) is followed by cessation of arc volcanism or migration of the arc front away from the trench. Mineralization in the central Altiplano-Puna region (21°–24°S) formed above a formerly flat subduction zone as volcanism was reinitiating. Thus, hydration and crustal thickening associated with transitions in and out of flat-slab subduction conditions are fundamental controls on formation of these major ore deposits.

INTRODUCTION

Some of the world's richest and largest copper and gold deposits are associated with Miocene magmatism in the central Andes. This paper reviews how the formation of major ore deposits between 22° and 34°S can be linked to the late Cenozoic magmatic and tectonic response of the mantle and lower crust to the formation and subsequent steepening of shallow subduction zones (Figs. 1 and 2). Mineral districts discussed are the El

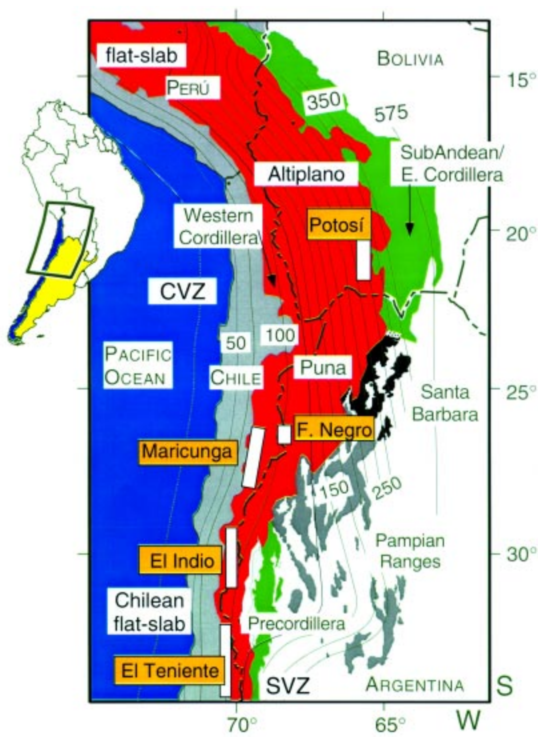

Figure 1: Central Andean map showing major Miocene mineralized areas (white boxes, yellow labels) relative to: (a) depth contours in km to Wadati-Benioff seismic zone of subducting Nazca plate (from Cahill and Isacks, 1992), (b) southern (SVZ) and central (CVZ) volcanic zones and Chilean and Peruvian flat-slab regions, (c) regions >3000 m in elevation (in red), and (d) foreland fold-thrust belts: Precordillera and Subandean–Eastern Cordillera thin-skinned belts (green), Santa Bárbara thick-skinned belt (black), and Pampean block uplifts (gray).

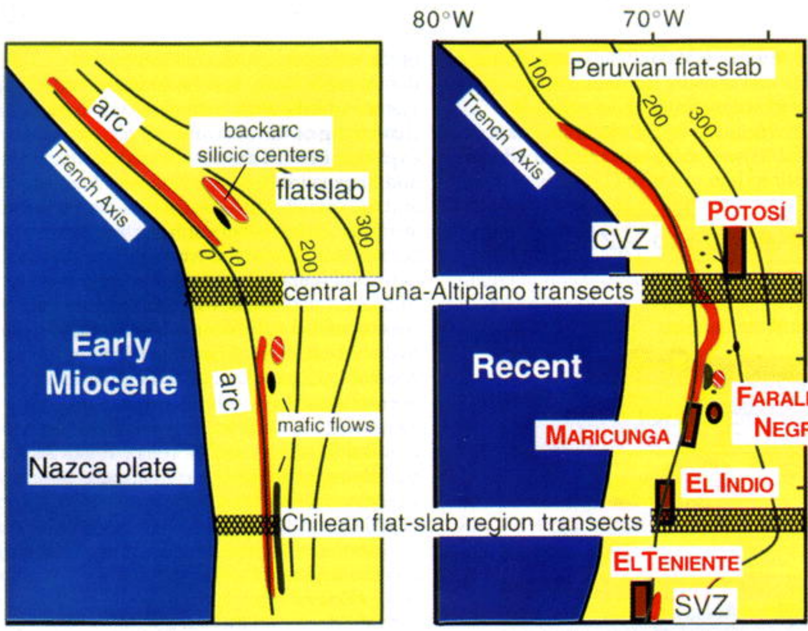

Figure 2: Early Miocene and Recent maps showing depth changes to Wadati-Benioff zone proposed by Isacks (1988) along with arc volcanic front (red), backarc mafic centers (black), and large ignimbritic centers (red stripes) from Kay et al. (1999). Miocene ore districts shown in brown boxes. Patterned bands are locations of reconstructed Miocene to Recent lithospheric cross sections in Figures 3 and 4.

Indio and Maricunga gold belts, the Farallon Negro copper-gold district, the El Teniente copper belt, and the Potosí silver-gold district. In the model, mineralization is linked to changes in crustal and lithospheric thickness induced by the evolving geometry of the subducting Nazca plate. Fluids for mineralization that are ultimately derived from the hydrated mantle above the subducting slab are released as wet amphibole-bearing lower crust thickens and transforms into dryer, garnet-bearing crust above a shallowing or recently shallow subduction zone. The model has implications for Miocene deposits over the shallow subduction zone in Peru and for Tertiary Laramide deposits in western North America.

TECTONIC SETTING OF MIOCENE CENTRAL ANDEAN ORE DEPOSITS

Major Miocene central Andean ore districts are located in extinct Miocene volcanic belts underlain by thickened continental crust (50–70 km thick; Isacks, 1988) on the arc side of major fold-thrust belts. This paper explores why they occur where they do. Figure 1 shows mineral districts between 22° and 34°S relative to modern central Andean geologic provinces and contours to the Wadati-Benioff seismic zone. The most prominent province, the Puna-Altiplano Plateau with its widespread Miocene to Recent volcanic cover and average elevation of 3700 m, is second on Earth only to the Tibetan Plateau in area and height. To the north and south, the Puna-Altiplano merges with the Main Cordillera of the high Andes. Most investigators attribute uplift and crustal thickening of the Puna-Altiplano and the Main Cordillera to Miocene crustal shortening with magmatic addition playing a secondary role (e.g., Isacks, 1988; Allmendinger et al., 1990, 1997). Prominent fold-thrust belts to the east provide a temporal record of this crustal shortening. These belts include the Subandean and Eastern Cordillera and Santa Bárbara Ranges east of the plateau, and the Precordillera and block-faulted Pampean Ranges east of the Main Cordillera.

A distinctive feature of the central Andes is the relatively shallow dip (<30°) of the subducting Nazca plate beneath South America compared to other circum-Pacific subduction zones. As recognized by Barazangi and Isacks (1976) and refined by Cahill and Isacks (1992), the Nazca plate can be divided at depths of ~90–135 km into nearly flat segments, above which there is no volcanism, that are flanked by relatively steeper segments associated with active volcanism (Fig. 1). The Chilean flat-slab segment between 28° and 33°S has a relatively smooth northern transition and an abrupt southern transition to the steeper segments (Fig. 1). In terms of this modern slab geometry, the El Indio belt is above the center of the Chilean flat slab, the Maricunga–Farallon Negro district above the northern transition, the El Teniente district above the southern transition, and the Potosí district above the steeper slab to the north.

Rationalizing the relationship among late Cenozoic central Andean uplift, crustal thickening, and Miocene mineralization requires understanding how the geometry of the subducting Nazca plate has changed since the breakup of the Farallon plate and the initiation of fast, nearly orthogonal convergence at ~26 Ma (Pardo Casas and Molnar, 1987). The model for evolving slab geometry used here is that proposed by Isacks (1988) on the basis of seismologic, structural and topographic constraints and modified by Kay et al. (1999) on magmatic considerations. The basic premise is that the slab beneath the modern shallow subduction zone has shallowed as the slab below the central Puna-Altiplano has steepened. Figure 2 compares the end-member early Miocene and modern situations, and Figures 3 and 4 show reconstructed lithospheric sections depicting the temporal evolution of transects through the Chilean flat slab and the Puna-Altiplano.

CHEMICAL CLUES TO TEMPORAL CHANGES IN MAGMATIC AND TECTONIC PROCESSES ASSOCIATED WITH MINERALIZATION

Important clues to processes occurring over a shallowing subduction zone come from magmas containing chemical components from the evolving slab, the overlying

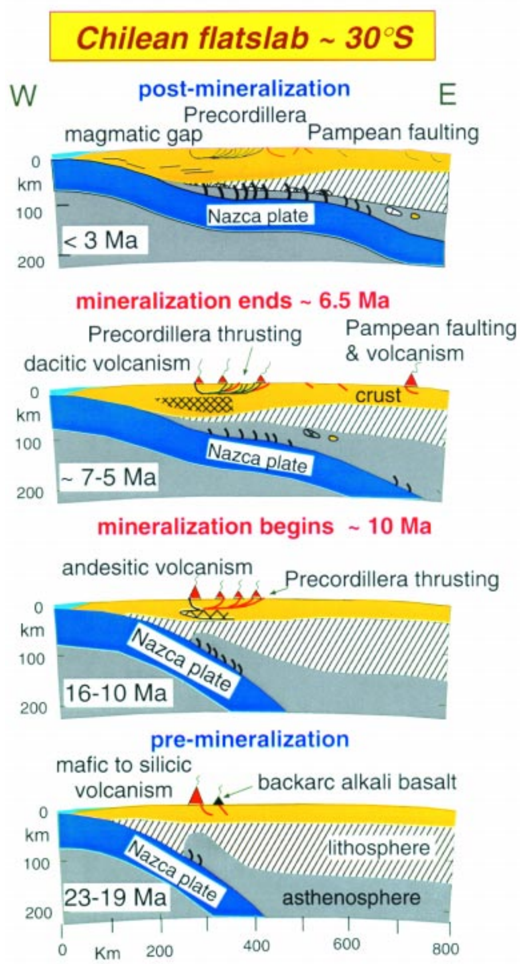

Figure 3: Schematic lithospheric cross sections across Chilean flat-slab transect at lat ~30ºS showing temporal changes in subducting slab geometry, crustal thickness, and areas of active volcanism and deformation before, during, and after mineralization. Size of volcanic centers reflect erupted volume. Hatched wedges represent areas of ductile thickening of the lower crust. Active faults shown in red. Figures based on Kay et al. (1991, 1999).

mantle wedge, and the crust. Uniquely, diagnostic chemical fingerprints can put restrictions on evolving temperature-pressure, chemical, and fluid profiles in the mantle and crust. Chemical analyses of more than 500 pre-, syn-, and postmineralization samples from the El Indio, Maricunga–Farallon Negro, and El Teniente districts all show the relatively high K, Ba, and Th, and low Ta concentrations expected in magmas erupted over a subduction zone (Kay et al., 1999). Central to the discussion below are the rare earth elements (REE), which show a relatively small range of La/Sm ratios and a wide range of Sm/Yb ratios (Fig. 5). Increasing Sm/Yb ratios mostly reflect pressure-dependent changes from clinopyroxene to amphibole to garnet in the mineral residue in equilibrium with evolving magmas (review in Kay and Kay, 1991). Following the proposition of Hildreth and Moorbath (1988) that arc magmas in a compressional regime evolve from mafic parent magmas in the lower crust and using Andean southern volcanic zone magmas and crustal thicknesses as depth indicators, Sm/Yb ratios can serve as guides to relative crustal thicknesses. Because breakdown pressures are influenced by factors like bulk composition and temperature, inferred depths are approximations. As a rough guide in mafic lavas, clinopyroxene is dominant at depths of <35 km, amphibole from ~30–45 km, and garnet at >45–50 km.

MAGMATISM, DEFORMATION, AND MINERALIZATION OVER A SHALLOWING SUBDUCTION ZONE

The lithospheric cross sections in Figure 3 illustrate a working model for the post–early Miocene shallowing of the Chilean subduction zone that accounts for magmatic, structural, and basin evolution over the modern flat-slab region and its borders (e.g., Kay et al., 1991, 1999; Jordan et al., 1993; Kay and Abbruzzi, 1996). Shallowing from ~18–8 Ma can account for decreasing amounts of volcanism and cessation of andesitic volcanism by ~9 Ma in the Main Cordillera, as well as an eastward broadening of the volcanic arc, the compressional deformation front, and the foreland basin system into the Precordillera. Continued shallowing of the slab after ~7 Ma can explain eastward expansion of deformation and magmatism into the Pampean Ranges, and the end of volcanism across the transect at ~5 Ma as the asthenospheric wedge became too thin in the west and the slab too dehydrated in the east to flux mantle melting. In concert with shallowing, the mantle and crust over the slab became increasingly hydrated under the Main Cordillera and the zone of hydration broadened eastward as decreasing asthenospheric circulation increasingly limited melting and fluid removal (e.g., Kay and Gordillo, 1994). As shallowing proceeded, magmatically weakened lower crust beneath the Main Cordillera thickened (Kay et al., 1991) in conjunction with crustal shortening in the Precordillera and the Sierras Pampeanas (e.g., Allmendinger et al., 1990), as well as with shortening in the forearc. Mass balance considerations require contemporaneous thinning of the continental lithosphere (Kay and Abbruzzi, 1996).

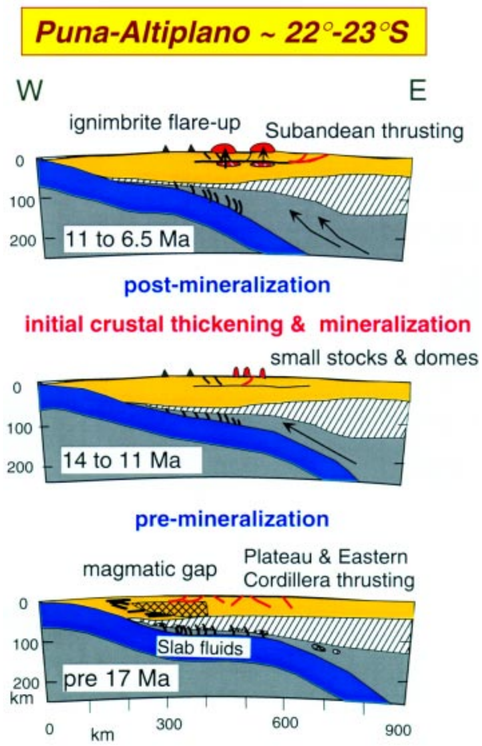

Figure 4: Schematic lithospheric cross sections along the central Puna-Altiplano Plateau transect lat ~22º–23ºS showing temporal changes in subducting slab geometry, crustal thickness and areas of active volcanism and deformation before, during, and after mineralization. Red striped regions are crustal magma chambers below master fault detachment that feed ignimbrites (in red). Figure based on Kay et al. (1999).

Important Miocene mineralization took place in the Chilean flat-slab region as the subduction zone was shallowing. Evidence for the temporal and spatial association between mineralization and Miocene magmatic stages and deformational events over the shallowing subduction zone beneath the El Indio, Maricunga–Farallon Negro, and El Teniente mineral districts is summarized in Table 1 and discussed below. Within the region, ages of mineralization, like average crustal thicknesses and subduction zone angles, decrease to the south and east.

The El Indio Transect. The El Indio transect is located in the Main Cordillera above the middle of the present flat slab. Major mineralization can be associated with the last two of three volcanic stages in this

TABLE 1. LATE OLIGOCENE TO RECENT TECTONIC, MAGMATIC, AND MINERALIZATION HISTORY OF THE CHILEAN FLAT-SLAB REGION

Ma	26°–28°S Maricunga Transect Thicker Crust	29°–31°S El Indio Belt Intermediate Thickness Crust	32°–34°S El Teniente District Thinner Crust
7–5	Flat-slab magmatism ends; arc migrates east on margins of flat slab; uplift, crustal thickening.		
	Au–Farallon Negro ~7–6 Ma	*Au–El Indio ~ends at ~6.5 Ma*	*Cu–El Teniente south ~4.9 Ma*
	Jotabeche dacite/Pircus Negras andesite	Vallecito Fm./ Vacas Heladas Ignimbrite	*Cu–Los Bronces ~7–5 Ma*
	(~60–65 km)	(~60 km)	(>45 km)
11–7	Silicic magmatism to north; last andesitic lavas in flat-slab region; andesitic stratovolcanoes to south.		
	Copiapó Ignimbrite Complex		
~17–9	Andesitic to dacitic stratovolcano complexes; Precordillera deformation and crustal thickening.		
	Au–Gold Porphyries ~12–10 Ma	*Au–El Indio ~begins at ~10 Ma*	*Cu-Pachon in north ~10–9 Ma*
	Cadillal Group	Tambo Formation ~13–9 Ma	El Teniente (Farallones Fm.)
	Ojos de Maricunga Group	Cerro de Las Tórtolas Fm. ~17–14 Ma	Volcanic/Plutonic Complex
	(>50 km)	(>45 km)	(~35-40 km)
20–18	Relative magmatic lull, deformation, and crustal thickening.		
26–20	Arc and backarc magmatism in all regions; more dacitic to andesitic in north; more bimodal to south.		
	Au–La Coipa-like domes ~23–21Ma	Las Máquinas backarc basalt ~23 Ma	
		Escabroso Formation ~21–17 Ma	Coya Machalí Formation
	Refugio/La Coipa Group (andesite)	Tilito Formation ~27–21 Ma	
	(~40–45 km)	(~35-40 km)	(~30–35 km)

Note: See Kay et al. (1999) for further references to these transects.

area. Each successive volcanic stage has a distinctive distribution and composition, shows a decrease in overall erupted volume, and is generally bounded by compressional deformational peaks (Kay et al.,1991, 1999). The initial Doña Ana Group is characterized by voluminous 27–21 Ma andesitic to rhyodacitic tuffs that unconformably underlie 21–17 Ma mafic andesite flows and are cut by small shallow intrusives (Martin et al., 1997). Small ~23 Ma (Las Máquinas) backarc alkali basalt flows are related to faults. Low-pressure pyroxene-bearing mineral residues complimentary to these magmas (Fig. 5; Kay et al., 1991) are consistent with ascent from lower levels of a normal thickness crust over a relatively steep subduction zone. This first volcanic stage terminated with high-angle reverse faulting in the Main Cordillera and initiation of thrust faulting in the Precordillera (Jordan et al., 1993). The second volcanic stage in the Main Cordillera is composed dominantly of ~17–14 Ma and ~13–9 Ma hornblende-bearing andesitic to dacitic units (Martin et al., 1997). Their REE patterns are consistent with equilibration in a thickening crust in which the mafic mineral residue changed from amphibole to garnet-bearing in the final stages (Fig. 5; Kay et al., 1991). This second stage also included small backarc amphibole-bearing andesitic to dacitic centers that extended into the Precordillera. The end of the second volcanic stage overlaps the peak of Precordillera thrust faulting at ~11–9 Ma (Jordan et al., 1993) and initiation of the major mineralization episode in the El Indio belt at ~10 Ma which lasted until 6.5 Ma (Clavero et al., 1997; Bissig et al., 2000). The terminal volcanic stage consists of minor ~7–6 Ma hornblende-bearing dacitic centers with amphibole-bearing residual mineralogy in the Main Cordillera (Vallecito in Fig. 5) and Precordillera, and mafic andesitic to dacitic centers in the Pampean Ranges (Kay and Gordillo, 1994).

The Maricunga Transect. Deformational and magmatic peaks in the Maricunga transect to the north near the boundary with the steeper slab are virtually analogous to those in the El Indio belt, but initial mineralization is older (Kay et al., 1994; Mpodozis et al., 1995). This mineralization at 23–21 Ma is linked to dacitic dome complexes emplaced near the end of a 26–21 Ma volcanic peak (Vila and Sillitoe, 1991; Mpodozis et al., 1995). Unlike first-stage El Indio magmas, REE patterns of these magmas point to amphibole-bearing lower crustal residues (Fig. 5) consistent with a thicker crust over a shallower subduction zone (see Fig. 2). This episode is followed by deformation and diminished volcanism from 20 to 18 Ma. Andesitic units that erupted at the beginning of the next volcanic stage from 17–12 Ma have steeper REE patterns consistent with a more garnet-rich residual mineralogy at deep levels of a thicker crust. In accord with this observation, regional uplift in the middle Miocene is signaled by thick sequences of alluvial sediments (Atacama gravels) which show syntectonic deformation east of the arc (Gardeweg et al., 1997). The second mineralization episode is linked to the emplacement of 13–10 Ma fault-controlled "gold porphyries" (e.g., Marte; Sillitoe et al., 1991) near the end of the second volcanic stage. REE patterns of these magmas again indicate an amphibole-bearing mineral residue. Mild extension and normal faulting at this time are consistent with models of stress relaxation during porphyry mineralization (Tosdal and Richards, 2001). The final stages of Maricunga belt volcanism are dominated by the ~11–7 Ma dacitic units from the Copiapó center, and 7–5 Ma Jotabeche rhyodacitic and Pircas Negras mafic andesitic flows. These postmineralization flows, which have REE patterns that indicate equilibration with garnet-bearing residues (Fig. 5), erupted through very thick crust as the arc front began to migrate eastward (Kay et al., 1999). The final mineralization in this transect at 7–6 Ma occurred in the Farallon Negro volcanic field to the east (Sasso and Clark, 1996), which erupted as volcanism migrated eastward and the crust thickened in association with uplift of the Pampean Ranges.

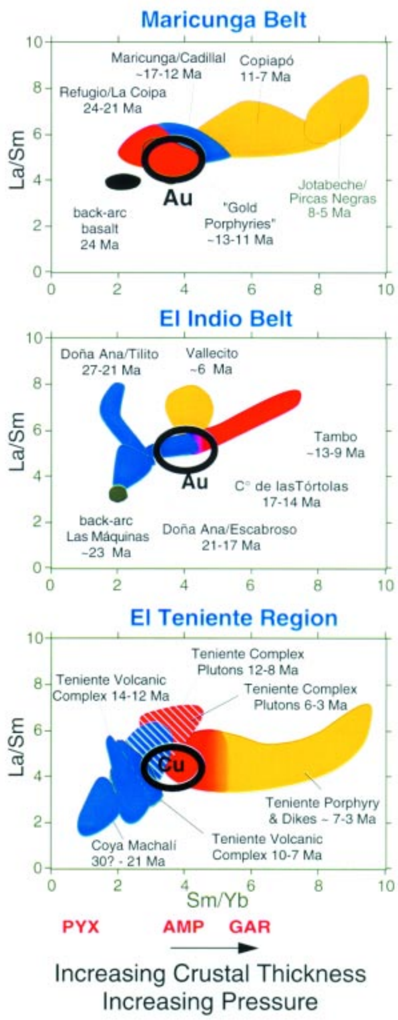

Figure 5: Plots of La/Sm (light REE) vs. Sm/Yb (heavy REE) ratios for more than 500 magmatic rocks from the Maricunga–Farallon Negro, El Indio, and El Teniente districts. Premineralization or between mineralization (Maricunga belt) units are in blue, synmineralization units in red, and postmineralization units in yellow. Hatched fields are plutonic units. Thick lines enclose fields for magmas erupted near times of gold (Au) and copper (Cu) mineralization. Presence of plutonic units and Cu rather than Au in the El Teniente district reflects greater erosion in this region. Samples in Au and Cu field have Sm/Yb ratios magmas in equilibrium with amphibole-bearing residual mineral assemblages in transition to garnet-bearing. Data sources in Kay et al. (1999) and Kay and Mpodozis (1999).

El Teniente Transect. El Teniente transect volcanism at the southern border of the flat-slab region also occurred in three stages separated by deformational peaks (Kurtz et al., 1997; Kay et al., 1999). Unlike the Maricunga transect, ages of shallowing of the subduction zone, crustal thickening, and mineralization are younger than in the El Indio belt. Voluminous mafic to silicic magmas of the first volcanic stage erupted through a thin crust in a neutral to slightly extensional tectonic regime. They were followed by an ~19–16 Ma lull associated with compressional deformation leading to initial uplift and crustal thickening (Kurtz et al., 1997). Magmatism resumed with the formation of the ~15–7 Ma Teniente volcanic and plutonic complex east of the older arc front. Like chemically equivalent early-to-middle Miocene El Indio belt magmas (Fig. 5), these premineralization Teniente Complex units have pyroxene to amphibole-dominated residual mineralogy. This magmatic stage ended with deformation (Godoy et al., 1999) and rapid regional uplift (~3 mm/year; Kurtz et al., 1997). Late Miocene to early Pliocene porphyries and dikes equilibrating with garnet-bearing residual assemblages (Fig. 5) were emplaced as the frontal volcanic arc south of 33°S shifted eastward to the present southern volcanic zone. Mineralization is associated with late Miocene tourmaline-bearing breccia complexes whose ages decrease from north to south: Pelambres–El Pachon deposit at 32°S at ~10–9 Ma, Rio Blanco–Los Bronces deposit at 33°S at ~7–5 Ma, and El Teniente deposit near 34°S at ~5 Ma (see Skewes and Stern, 1994, 1997). Skewes and Stern (1994) argue that metal-rich fluids forming these deposits are released as long-lived plutons cool and solidify in the dying magmatic arc over the shallowing subduction zone.

MAGMATISM, DEFORMATION, AND MINERALIZATION OVER A FORMERLY SHALLOW SUBDUCTION ZONE

Important central Andean Miocene mineralization also occurred in the northern Puna and southern Altiplano near 21°–23°S in an area where the present slab dip is steep

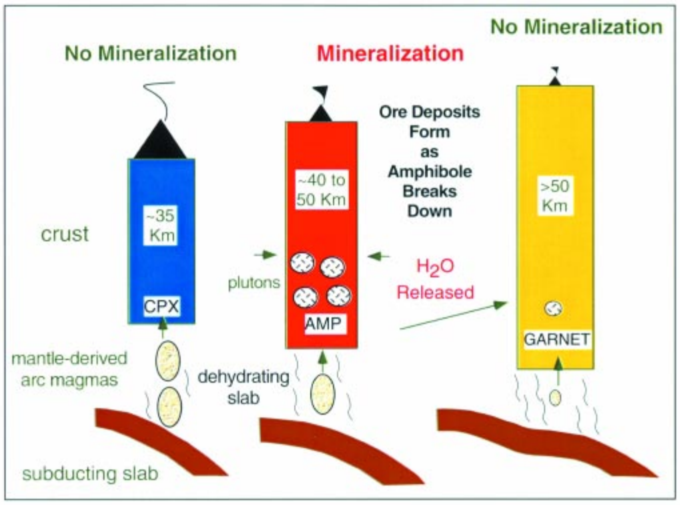

Figure 6: Cartoon showing genetic model for major Miocene central Andean ore districts. Stage 1 shows magmas equilibrating with pyroxene-bearing mineral residues in normal thickness continental crust over relatively steep subduction zone. Stages 2 and 3 show magmas equilibrating with amphibole-bearing and garnet-bearing mineral residues in deep parts of thickening crust over shallowing subduction zone. Mineralization occurs between stages 2 and 3. Critical ingredients are a hydrated mantle above a shallow subduction zone, storage of fluid in amphibole and hydrous magmas in the deep crust, and release of that fluid in conjunction with breakdown of amphibole-bearing crustal assemblages in crustal melt zones during subhorizontal shortening and thickening of ductile, magma-injected crust.

(Fig. 1). This mineralization is associated with a group of 14–12 Ma stocks and domes, and includes the giant silver deposit in the Cerro Rico de Potosí stock (13.8 Ma; Zartman and Cunningham, 1995). Lithospheric cross sections from 18 to 7 Ma in Figure 4 for the transect show the distribution of volcanism and deformation, slab geometries, and crustal thicknesses proposed by Kay et al. (1999). The existence of an early-to-middle Miocene shallow subduction zone (Fig. 2) is consistent with a volcanic gap (Coira et al., 1993) associated with widespread late Oligocene–early Miocene deformation in the southern Altiplano (Allmendinger et al., 1997). As in the modern Chilean flat-slab region, a thin asthenospheric wedge is interpreted to have inhibited arc magmatism while enhancing mantle hydration above a shallowly subducting slab (James and Sacks, 1999). Steepening of the slab in the middle Miocene increased the volume of the asthenospheric wedge promoting melting of the overlying hydrated mantle and lower crust. Heating of the crust by mantle-derived magmas in a compressional regime provides a mechanism for ductile thickening of the lower crust and plateau uplift. Mineralization at ~14–12 Ma appears to be associated with the first “wet” magmas erupted as the slab steepened and the crust thickened. Continued crustal thickening accompanied eruption of huge late Miocene plateau ignimbrite sheets as brittle deformation terminated under the plateau region and upper crustal deformation migrated eastward. Plateau uplift accompanied Subandean Belt thrusting as both movement on thrusts and large ignimbrite eruptions were triggered by horizontal compressional collapse of the melt-weakened crust. Subsequent volcanism was progressively concentrated to the west as the slab continued to steepen and the lithosphere thickened in response cooling and underthrusting of the Brazilian shield (Allmendinger et al., 1997). No major mineralization is associated with post-10 Ma volcanic units in the transect (Coira et al., 1993).

MODEL FOR MINERALIZATION OVER A SHALLOWING SUBDUCTION ZONE AND A THICKENING CRUST

The discussion above shows that common features of giant Miocene Andean ore deposits include formation over a shallowing or formerly shallow subduction zone in a thickened crust near the end or at the beginning of a volcanic episode. Magmas erupted near times of mineralization are in equilibrium with an amphibole-bearing mafic mineral residue that is changing to garnet. These features are incorporated in the general model in Figure 6 which builds on long-standing ideas of associating these deposits with hydrous magmas over subduction zones (e.g., Barnes, 1997).

Linking mineralization with a shallowing (or formerly shallow) subduction zone over a thickening crust is important as decreasing mantle flow in the cooling wedge above the dehydrating, shallowing slab increasingly limits melting and fluid removal from the wedge. Melts entering the thickening lower crust from this wedge become increasingly hydrous as fluids are progressively concentrated in the cooling mantle. As shown in stage 1 of Figure 6, arc magmas erupted through a normal thickness crust before the slab shallows have anhydrous residual mineral assemblages and are not linked to large ore deposits. In contrast, arc magmas formed above the cooling, hydrating mantle in stage 2 of Figure 6 contain fluids that cause amphibole to crystallize in them as they are underplated and intruded into a thickening crust. This process can occur for as much as 6–8 m.y. before mineralization as shown by eruption of amphibole-bearing Miocene lavas in the El Indio and El Teniente belts.

An implication for mineralization is that breakdown of amphibole can release a significant amount of fluid during melting resulting in hydrous magmas. Fluid can come from amphibole in underplated magmas and their cumulate and melt residues, as well as from metamorphosed amphibole-bearing lower crustal units. These fluids can be liberated as magma are emplaced and cooled in shallow level magma chambers. Oxidizing conditions, which prevent the early removal of sulfide minerals and allow metals to be concentrated in the residual fluids of crystallizing magmas are consistent with trace-element signatures (e.g., small Eu anomalies with low Sr contents; see Kay et al., 1991, 1999).

The observation that major central Andean Miocene ore deposits generally form near the end of a deformational peak in a setting where compression leads to crustal shortening and thickening highlights a role for thickened crust in the breakdown of hydrous minerals. REE patterns of silicic melts from the lower crust are the best indicators of the change from intermediate pressure, hydrous amphibolite/garnet amphibolite to high-pressure dry granulite/eclogite metamorphic facies residues. Sm/Yb ratios of samples in Figure 5 indicate that major periods of central Andean Miocene mineralization occurred as the mafic mineral residue changed from hornblende to garnet. Garnet-dominated signatures are present in most postmineralization silicic magmas erupted in the Maricunga, El Teniente, and El Indio belts. Major ore deposits are not found associated with magmas like those in stage 3 of Figure 6 as their anhydrous garnet-dominated mafic mineral residues lack adequate fluid sources.

Another essential factor linking fluid sources associated with ore deposits to tectonic stresses is that magmas intruding a thickened crust under compression have difficulty ascending and evolve at depth leading to high intrusive/extrusive ratio magmatic systems. Storage at depth promotes repeated crustal melting, enhances crustal ductility, and makes the crust susceptible to horizontal compressional failure leading to crustal shortening and thickening. Such conditions promote pressure-induced amphibole breakdown in lower crustal melt zones. Multiple melt and freeze cycles in these melt zones could enhance metal enrichment. The erupted magmas are a combination of crustal and mantle components that last equilibrated with lower crustal mineral residual assemblages. This is essentially the MASH process of Hildreth and Moorbath (1988). The importance of uplift and solidification of long-lived magmatic systems to metal-rich fluid release over a shallowing subduction zone is addressed for the El Teniente district by Skewes and Stern (1994). Temporal coincidence of ductile crustal thickening beneath the arc and upper crustal shortening in the backarc is evident in the Chilean flat slab (e.g., Kay and Abbruzzi, 1996), and has been proposed for the El Teniente (e.g., Kurtz et al., 1997; Godoy et al., 1999) and Maricunga (Kay et al., 1994) transects.

Crustal thickening due to shortening must also be compensated in the lithospheric mantle. Thickening of the lithosphere reduces space for the asthenospheric wedge above the shallowing slab and forces retreat of the melt zone towards the backarc. As such, a thicker crust and a shallower slab under the El Indio belt than under the Maricunga and El Teniente belts can account for volcanic quiescence in the former, and eastward migration of the frontal arc in the latter. An unresolved question is the role of subduction erosion (forearc removal of the hanging wall of the plate above the subduction zone) and the mechanical removal of basal continental lithosphere and continental crust in the arc and backarc as the subduction zone shallows and the crust thickens. Such lithospheric thinning allows for the return of a thickened asthenospheric wedge renewing magma production above the slab, and could be important in explaining multiple mineralization episodes such as those in the Maricunga and El Indio belts.

TIMING OF TECTONIC AND MINERALIZATION EVENTS

Mineralization events generally correspond to crustal deformational peaks which can be argued to be approximately contemporaneous along the Andean front from Peru to Chile. Sébrier and Soler (1991) suggest that peaks near ~17 Ma, ~10 Ma, ~7 Ma, and ~2 Ma occurred at times of little or no westward retreat of the subducting Nazca plate relative to South America. Such a regime could be related to changes in plate directions and spreading rates. Whether mineralization occurs in a given place depends on local crustal thickness, asthenospheric wedge volume, and the geometry of the subducting plate. This unifying model links mineralization to the changing dip of shallow subduction zones beneath continents.

ACKNOWLEDGMENTS

Discussions with R.W. Kay, B. Coira, V.A. Ramos, and E. Godoy are especially acknowledged. Funding came from the National Science Foundation (EAR89-03732, 92-05042), CODELCO, Chilean SERNAGEOMIN and FONDECYT (1950025, 1990009), and Argentine Geologic Survey. Review by Jeremy Richards and Karl Karlstrom improved the presentation.

REFERENCES CITED

Allmendinger, R.W., Figueroa, D., Snyder, D., Beer, J., Mpodozis, C., and Isacks, B.L., 1990, Foreland shortening and crustal balancing in the Andes at 30°S latitude: Tectonics, v. 9, p. 789–809.

Allmendinger, R.W., Jordan, T.E., Kay, S.M., and Isacks, B.L., 1997, The evolution of the Altiplano-Puna Plateau of the central Andes: Annual Reviews of Earth and Planetary Science, v. 25, p. 139–174.

Barazangi, M., and Isacks, B.L., 1976, Spatial distribution of earthquakes and subduction of the Nazca plate beneath South America: Geology, v. 4, p. 686–692.

Barnes, H.L., 1997, Geochemistry of Hydrothermal Ore Deposits: New York, John Wiley & Sons, 972 p.

Bissig, T., Clark, A.H., Lee, J.K.W., and Heather, K.B., 2000, Revised metallogenetic model for the El Indio–Pascua/Lama Au (Ag, Cu) belt, Regiones III/IV, Chile and Provincía San Juan, Argentina: GSA Abstracts with Programs, v. 32, p. A372.

Cahill, T.A., and Isacks, B.L., 1992, Seismicity and shape of the subducted Nazca plate: Journal of Geophysical Research, v. 97, p. 17,503–17,529.

Clavero, J.R., Martin, M.W., Mpodozis, C., and Cultiño, L., 1997, Eventos alteración-mineralización en la franja el Indio (29°–30°S), nuevos antecedentes geológicos y geochronológicos: Antofagasta, Chile,VIII Congreso Geológico Chileno Actas 2, p. 896–900.

Coira, B., Kay, S.M., and Viramonte, J., 1993, Upper Cenozoic magmatic evolution of the Argentine Puna—A model for changing subduction geometry: International Geology Review, v. 35, p. 677–720.

Gardeweg, M., Mpodozis, C., Clavero, J., 1997, Hoja Ojos del Salado, Mapas Geológicos (1:100 000): Servicio Nacional de Geología y Minería, open file, Santiago, Chile.

Godoy, E., Yanez, G., and Vera, E., 1999, Inversion of an Oligocene volcano-tectonic basin and uplifting of its superimposed Miocene magmatic arc in the Chilean central Andes; first seismic and gravity evidence: Tectonophysics, v. 306, p. 216–236.

Hildreth, W., and Moorbath, S., 1988, Crustal contributions to arc magmatism in the Andes of central Chile: Contributions to Mineralogy and Petrology, v. 98, p. 455–489.

Isacks, B.L., 1988, Uplift of the central Andean plateau and bending of the Bolivian orocline: Journal of Geophysical Research, v. 93, p. 3211–3231.

James, D.E., and Sacks, J.W., 1999, Cenozoic formation of the central Andes: A geophysical perspective, *in* Skinner, B., ed., Geology and ore deposits of the central Andes: Society of Economic Geology Special Publication 7, p. 1–25.

Jordan, T.E., Allmendinger, R.W., Damanti, J., and Drake, R., 1993, Chronology of motion in a complete thrust belt: The Precordillera, 30°–31°S, Andes Mountains: Journal of Geology, v. 101, p. 133–156.

Kay, R.W., and Kay, S.M., 1991, Creation and destruction of lower continental crust: Geologische Rundschau, v. 80, p. 259–278.

Kay, S.M., and Abbruzzi, J.M., 1996, Magmatic evidence for Neogene lithospheric evolution of the central Andean "flat slab" between 30° and 32°S: Tectonophysics, v. 259, p. 15–28.

Kay, S.M., and Gordillo, C.E., 1994, Pocho volcanic rocks and the melting of depleted continental lithosphere above a shallowly dipping subduction zone in the central Andes: Contributions to Mineralogy and Petrology, v. 117, p. 25–44.

Kay, S.M., and Mpodozis, C., 1999, Setting and origin of Miocene giant ore deposits in the central Andes: PACRM'99, The Australasian Institute of Mining and Metallurgy Publication Series 44, p. 5–12.

Kay, S.M., Mpodozis, C., and Coira, B., 1999, Magmatism, tectonism, and mineral deposits of the central Andes (22°–33°S), *in* Skinner, B., ed., Geology and ore deposits of the central Andes: Society of Economic Geology Special Publication 7, p. 27–59.

Kay, S.M., Mpodozis, C., Ramos, V.A., and Munizaga, F., 1991, Magma source variations for mid-late Tertiary magmatic rocks associated with a shallowing subduction zone and a thickening crust in the central Andes (28° to 33°S) Argentina, *in* Harmon, R.S., and Rapela, C.W., eds., Andean magmatism and its tectonic setting: Boulder, Colorado, Geological Society of America Special Paper 265, p. 113–137.

Kay, S.M., Mpodozis, C., Tittler, A., and Cornejo, P., 1994, Tertiary magmatic evolution of the Maricunga mineral belt in Chile: International Geology Review, v. 36, p. 1079–1112.

Kurtz, A., Kay, S.M., Charrier, R., and Farrar, E., 1997, Geochronology of Miocene plutons and Andean uplift history in the El Teniente region, central Chile (34°–35°S): Revista Geológica de Chile, v. 24, p. 75–90.

Martin, M., Clavero, J., and Mpodozis, C., 1997, Eocene to Late Miocene magmatic development of the El Indio belt, ~30°S, north-central Chile: Antofagasta, Chile, VIII Congreso Geológico Chileno Actas 1, p. 149–153.

Mpodozis, C., Cornejo, P., Kay, S.M., and Tittler, A., 1995, La Franja de Maricunga: Sintesis de la evolución del frente volcánico oligoceno-mioceno de la zona sur de los Andes Centrales: Revista Geológica de Chile, v. 22, p. 273–314.

Pardo-Casas, F., and Molnar, P., 1987, Relative motion of the Nazca (Farallon) and South American plates since Late Cretaceous time: Tectonics, v. 6, p. 233–248.

Sasso, A., and Clark, A.H., 1998, The Farallon Negro group, northwest Argentina: Magmatic, hydrothermal, and tectonic evolution and implications for Cu-Au metallogeny in the Andean backarc: Society of Economic Geology Newsletter, v. 34, p. 1–18.

Sébrier, M., and Soler, P., 1991, Tectonics and magmatism in the Peruvian Andes from late Oligocene time to the present, *in* Harmon, R.S., and Rapela, C.W., eds., Andean magmatism and its tectonic setting: Boulder, Colorado, Geological Society of America Special Paper 265, p. 259–279.

Sillitoe, R.H., McKee, E.H., and Vila, T., 1991, Reconnaissance K-Ar geochronology of the Maricunga gold-silver belt, northern Chile: Economic Geology, v. 86, p. 1261–1270.

Skewes, M.A., and Stern, C.H., 1994, Tectonic trigger for the formation of late Miocene Cu-rich megabreccias in the Andes of central Chile: Geology, v. 22, p. 551–554.

Skewes, M.A., and Stern, C.H., 1997, Late Miocene mineralized breccias in the Andes of central Chile: Sr- and Nd-isotopic evidence for multiple magmatic sources, *in* Camus, F., et al., eds., Society of Economic Geology Special Publication 6, p. 551–554.

Tosdal, R., and Richards, J.P., 2001, Magmatic and structural controls on the development of porphyry Cu±Mo ±Au deposits: Reviews in Economic Geology, v. 14, (in press).

Vila, T., and Sillitoe, R.H., 1991, Gold-rich porphyry systems in the Maricunga belt, northern Chile: Economic Geology, v. 86, p. 1238–1260.

Zartman, R.E., and Cunningham, C.G., 1995, U-Th-Pb zircon dating of the 13.8 dacite volcanic dome at Cerro Rico de Potosí, Bolivia: Earth and Planetary Science Letters, v. 133, p. 227–237.

Manuscript received October 10, 2000; accepted January 4, 2001. ▲